Immunometabolic Profiling of Enteric Glial Cells in Response to Acute and Chronic Pro-Inflammatory Cytokine Exposure: Implications for Early Pathogenic Insights into Parkinson's Disease

Alexandra-Ioana Matei

Major Research Internship Report

MSc Drug Innovation

Daily supervisor: Anastasia Markidi, MSc

Examiners: Dr. P. Perez Pardo & Prof. dr. C.R. Berkers

Utrecht University
December 2023

Table of Contents

Layman’s Summary

Parkinson’s disease (PD) is a chronic degenerative disorder that affects the dopamine-producing neurons in a specific brain region called substantia nigra. The characteristic symptoms of PD are movement-related (motor) symptoms such as tremors of limbs, slowness of movement, limb stiffness, and balance problems. Recently, research has shown that patients with PD experience symptoms unrelated to movement years before the onset of the characteristic motor symptoms. Such symptoms include depression, reduced ability to smell, changes in memory and thinking ability, sleep disorders, constipation, or digestive issues. Out of these non-motor symptoms, issues related to the digestive system are most commonly experienced by PD patients. This led scientists to study the relation between these gastrointestinal issues and the onset of PD. Recent research suggests that the health of our gut can affect our brain through the connection between the gut microbes and the brain, named the gut-brain axis. The enteric nervous system (ENS), often called the brain in the gut, is a complex network of neurons and glial cells found in the gut wall. These cells can interact with the immune system and gut microbes and maintain a healthy balance in the gut (homeostasis). The microbial populations in the gut (gut microbiome) can be influenced by ageing, diet and antibiotic usage, leading to changes in the protective roles of the microbiome. As a result, changes in the structure of the intestinal walls can occur, resulting in increased intestinal permeability. This condition is commonly referred to as "leaky gut". The changes in the gut wall structure make it easier for harmful bacteria to get through and cause local inflammation. Enteric glial cells (EGCs) are a type of cell that support the roles of neurons in the gastrointestinal tract. They can be activated and respond to inflammation by aiding the resolution of the inflammation. Currently, the treatment of Parkison is purely symptomatic; therefore, understanding the early development of Parkinson's disease is essential for discovering new therapies that could stop the development or progression of the disease. In this study, we aim to look at the effects of long-term exposure to pro-inflammatory stimuli on the immune and metabolic functions of EGCs.

Abstract

Parkinson’s disease (PD) is a widespread neurodegenerative disorder characterised by the presence of α-syn aggregates, which have been associated with the degeneration of dopaminergic neurons in the substantia nigra pars compacta (SNpc). Recent studies have shown that the intestinal environment's state can modulate the central nervous system (CNS) activity via the microbiota-gut-brain axis. Gut microbes can modulate immune and inflammatory events in the gut and trigger neuroinflammation and subsequent neurodegeneration. The enteric nervous system (ENS) is a complex network of enteric neurons and glia that can interact with the gut immune system and microbiome. Enteric glial cells (EGCs) are peripheral neuroglia associated with processes of enteric neurons in the gastrointestinal tract. EGCs can be activated and respond to proinflammatory stimuli, amplifying the inflammatory response. Studying the metabolism of EGCs in response to a long inflammation may provide new insights into the pathophysiology of neurodegenerative disorders. In this study, hESC-derived ENS cells, based on the protocol of Gogolou et al., will be used to investigate the immuno-metabolic effects of (i) acetate on the inflammation induced by pro-inflammatory stimuli, either LPS or a cytokine mix (TNF-α & IL-1β), and of (ii) chronic exposure to pro-inflammatory stimuli. LPS stimulation failed to induce inflammation in our system due to the absence of the TLR4 receptor on the cell surface of EGCs. Acetate failed to suppress inflammation following exposure to a pro-inflammatory cytokine mix. Following chronic pro-inflammatory cytokine exposure, levels of IL-6 in the first 48h were increased and steadily decreased throughout the experiment. Levels of IL-8 follow a similar trend to IL-6 release, however, the decrease is not as significant as with IL-6. Preliminary results show the presence of p129syn in the soma of the neurons following chronic exposure to pro-inflammatory cytokines. Glucose uptake is increased in cytokine-treated cells on day 2, suggesting a significant impact on metabolic processes by promoting a metabolic shift towards glycolysis. Intracellular metabolism indicates that long-term exposure to pro-inflammatory cytokines induced a major change in the EGCs' metabolic phenotype. Pathway analysis shows that after 14 days, between controls and cytokine-treated cells, multiple metabolic pathways are significantly altered. These preliminary observations of the effects of chronic pro-inflammatory cytokine exposure could be used to develop potential therapeutic targets for gut inflammation and to understand early PD pathogenesis and progression.

Keywords: Parkinson’s disease, hESCs, Enteric Nervous System, α-syn, SCFAs, TNF-α, IL-1β, inflammation, gut-brain-axis

List of Abbreviations

ATP	Adenosine Triphosphate
BSA	Bovine Serum Albumin
CNS	Central Nervous System
EGCs	Enteric Glial Cells
ENS	Enteric Nervous System
ELISA	Enzyme-Linked Immunosorbent Assay
GFAP	Glial Fibrillary Acidic Protein
GI	Gastrointestinal
hESCs	Human-Embryonic Stem Cells
IL-1β	Interleukin-1 beta
IL-4	Interleukin-4
IL-6	Interleukin-6
IL-8	Interleukin-8
LPS	Lipopolysaccharides
NGS	Normal Goat Serum
NMS	Non-Motor Symptoms
NO	Nitric Oxide
OCT3/4	Octamer Binding Transcription Factor 3/4
p-α-syn/p129syn	Phosphorylated A-Synuclein
PBS	Phosphate-Buffered Saline
PCA	Principal Component Analysis
PD	Parkinson’s Disease
SCFAs	Short-Chain Fatty Acids
SNpc	Substantia Nigra Pars Compacta
TCA	Tricarboxylic Acid Cycle
TLRs	Toll- Like Receptors
TLR4	Toll- Like Receptor 4
TNF-α	Tumor Necrosis Factor Alpha
TUJ-1	Neuron-Specific Class III Beta-Tubulin
α-syn	Alpha-Synuclein

1 | Introduction

1.1 | Parkinson's Disease

Parkinson's disease (PD) affects around 6.1 million people worldwide, making it the second most common neurodegenerative disorder, after Alzheimer's disease (1,2). PD is a complex neurodegenerative disorder characterised by the death of dopaminergic neurons in the substantia nigra pars compacta (SNpc) region in the brain. The reasons for the onset of neurodegeneration are still unknown however research shows that environmental and genetic factors might be involved in the pathogenesis of PD (3).

Parkinson's disease is characterized by motor symptoms such as bradykinesia, tremor, rigidity, and later postural instability (4). However, it is currently believed that PD may have a long prodromal phase, starting years prior to the manifestation of the hallmark motor symptoms. Non-motor symptoms (NMS) including depression, hyposmia, cognitive impairment, sleep disorders, or constipation can precede neurodegenerative conditions, including PD, by several years (5,6).

The neuropathological feature of PD is the presence of misfolded and aggregated α-synuclein (α-syn) in the form of Lewy bodies (7). The aggregation of α-syn has been associated with the dysfunctionality and degeneration of dopaminergic neurons. It is important to note that certain post-translational modifications, such as phosphorylation, can contribute to the misfolding and aggregation of α-syn. Approximately 90% of the α-syn present in Lewy bodies is phosphorylated, suggesting a close relationship between phosphorylation at S129 (p129syn) and α-syn aggregation in PD (8,9). Moreover, oxidative stress could also play an important role in the aggregation of α-syn and neurodegeneration by contributing to nitric oxide toxicity and inflammation (10).

1.2 | The Gut-Brain-Axis and Gut Microbiota

Despite the presence of misfolded and aggregated α-syn in the SNpc being a key finding in PD, recent evidence suggests that α-syn pathology starts in the gastrointestinal (GI) tract, and then spreads to the central nervous system (CNS) via the gut-brain axis. In the study conducted by Van Den Berge et al. the authors show that in rat models, duodenal injection of preformed α-syn fibrils results in the spread of α-syn to the brainstem and the stomach (11). Similarly, the spread of α-syn fibrils to different regions of the brain, was demonstrated by injection of α-syn fibrils into the duodenal and pyloric muscular layer (12). These studies provide evidence to support the hypothesis that α-syn propagates from the GI tract to the CNS via the vagus nerve. What is more, it has been reported that in mouse models, exposure to pro-inflammatory stimuli caused an increase in α-syn expression in the large intestine and expression of p129syn in colonic myenteric neurons before the appearance of the hallmark motor symptoms and prior to nigrostriatal degeneration (13). These findings suggest that PD may originate in the GI tract and spread to the brain through the via the brain-gut axis.

The initiation of PD at a gut level is supported by GI symptoms being present years prior to the manifestation of the hallmark motor symptoms. GI dysfunction, increased gut permeability, and gut microbiota alterations, also known as dysbiosis, are some of the most common NMS observed in PD patients (14). The gut microbiota is highly dynamic and can be altered by ageing, diet and antibiotic usage. Modifications in the gut microbiota can lead to changes in the protective roles of the microbiome (processing dietary fibres, protecting against pathogens,

and regulating metabolic endocrine and immune functions) resulting in high intestinal permeability, named “leaky gut” (15,16).

The disrupted intestinal epithelium allows enteric pathogenic bacteria and bacterial metabolites, such as lipopolysaccharides (LPS) to translocate and induce local inflammation. Increased amounts of pathogenic bacteria cause the overactivation of Toll-like receptors (TLRs), which in turn causes an overexpression of pro-inflammatory cytokines and subsequent epithelial damage and chronic inflammation (17). The released pro-inflammatory factors and activated immune cells can translocate in to the systemic circulation and reach the CNS. Once present in the CNS, pro-inflammatory cytokines can trigger neuroinflammation and subsequent neurodegeneration (18). In turn, neuroinflammation in the CNS can enhance enteric inflammation, creating a positive loop leading to a chronic state of neuroinflammation which is believed to play a crucial role in the progression of PD (19).

1.3 | The Enteric Nervous System and Enteric Glial Cells

The entric nervous system (ENS) is a complex network of enteric neurons and glia, arranged in networks of enteric ganglia that spread out through the GI tract (20). Due to its proximity to the GI tract, the ENS can interact with the gut immune system and microbiome and regulate tissue homeostasis and pathogen defence (15,21). Enteric glial cells (EGCs) are essential for modulating gut functions by creating an interplay between neurons, epithelial and immune cells. Upon exposure to pro-inflammatory stimuli, EGCs can be activated and subsequently release pro-inflammatory cytokines, glial cell-derived neurotrophic factors, and other immunomodulatory signalling molecules. Moreover, activated EGCs can trigger the activation of immune cells which amplifies the pro-inflammatory environment and intestinal barrier damage. Depending on their activation state, EGCs are susceptible to phenotypic changes, ranging from a proinflammatory neurotoxic profile to an anti-inflammatory neuroprotective phenotype. The dynamic response of EGCs to pro-inflammatory stimuli, characterized by their ability to modulate immune responses and the potential for phenotypic changes, underscore the ENS as a key regulator in the complex network governing intestinal homeostasis (22).

1.4 | Short Chain Fatty Acids

Short-chain fatty acids (SCFAs) are the main products of fermentation of dietary fiber and have been suggested to have an anti-inflammatory function. SCFAs excert their anti-inflammatory properties by suppressing the production of pro-inflammatory mediators including Tumor Necrosis Factor-α (TNF-α), Interleukin-1β (IL-1β), Interleukin-6 (IL-6), and nitric oxide (NO). Moreover, SCFAs can increase the release of anti-inflammatory cytokines, like Interleukin-10 (IL-10) (23). Interestingly, a study by Unger et al. showed fecal SCFA concentrations were significantly reduced in PD patients compared to controls (24). Further investigations into the intricate interplay between SCFAs and resolution of inflammation may offer valuable insights for developing targeted therapeutic strategies in Parkinson's disease.

This study aims to investigate the immunometabolic effects of (i) acetate on the inflammation induced by pro-inflammatory stimuli, either LPS or a cytokine mix, and (ii) long-term exposure to pro-inflammatory stimuli on an *in vitro* ENS model. This will be achieved by looking at signs of immune activation in the ENS cell culture supernatant and by studying the change in the metabolism of EGCs. Generation of the *in vitro* ENS cells was done following the differentiation protocols using hESCs, developed by Gogolou et al. (25).

2 | Methods

2.1 | Culture of human embryonic stem cells (hESCs)

H1 human embryonic stem cells (H1-hESCs) were kindly provided by Dr. Massimiliano Caiazzo (Utrecht University). Cells were cultured in Essential 8™ medium (E8, Gibco™) on Matrigel® matrix (Corning®, USA) coated 6-well flat-bottom cell culture microplates (Corning®, USA). Cells were kept in a humidified cell culture incubator with 5% CO_2 at 37°C. Cells were passaged when 80-85% confluency was reached by exposure to 0.001% EDTA in PBS for 2-3 minutes at 37°C, 5% CO_2. The EDTA solution was carefully aspirated, and pre-warmed E8 medium was added to carefully detach the cells. Further, the desired cell fraction was plated onto newly coated Matrigel plates.

2.2 | Generation of the *in vitro* Enteric Nervous System

2.2.1 | Generation of vagal neural crest cells or early ENS progenitors

hESCs were detached into single cells by exposure to Accutase for 5-7 minutes at 37°C, 5% CO_2. Accutase was then neutralised with DMEM:F12, and cells were transferred into a conical centrifuge tube and spined 300g for 4 minutes at room temperature to allow for the careful removal of the supernatant. The cell pellet was carefully resuspended in Neural Crest Induction Medium (Table 1A) before counting the cells using a hemocytometer. Cells were plated at 20.000 cells/cm^2 density on a Matrigel® matrix (Corning®, USA) coated 6-well flat-bottom cell culture microplate (Corning®, USA). Cells were moved back and forth, side to side, to ensure even distribution of the cells and then incubated at 37°C in a humidified atmosphere with 5% CO_2. Medium changes were performed on days 2, 4 and 5 by aspirating the old medium and adding freshly prepared Neural Crest Induction Medium.

2.2.2 | Generation of Enteric Neurons and Glia

The previously cultured vagal neural crest cells were used to generate the formation of 3D cell sphere aggregates that were further used to generate enteric neurons and glia. The medium from day 6 was aspirated, and PBS was added to wash the cells. Vagal neural crest cells were lifted into single-cell suspension by exposure to Accutase for 5-7 minutes at 37°C, 5% CO_2. Following incubation, Accutase was neutralised with DMEM:F12 and cells were transferred into a conical centrifuge tube and spined 300g for 4 minutes at room temperature to allow for the careful removal of the supernatant. The cell pellet was carefully resuspended in Complete Sphere Culture Medium (Table 1B) before being transferred to 6-well ultra-low attachment plates and centrifuged at 100g for 2 minutes at room temperature. Cells were incubated at 37°C in a humidified atmosphere with 5% CO_2. Half medium change was performed on day 8. On day 9, spheres were replated into poly-L-ornithine and Matrigel® coated 6-well flat-bottom cell culture microplates (Corning®, USA). Half medium changes were performed every other day for the remaining days of the differentiation by removing half of the old medium and replacing it with freshly prepared Complete ENS Culture Medium (Table 1C). Cells were incubated at 37°C in a humidified atmosphere with 5% CO_2.

Table 1 – Composition of used culture mediums

A. Neural Crest Induction Medium

Ingredient	Final concentration	Supplier and Catalogue number
DMEM/F12	Not applicable	Thermo Fisher Scientific, 21331020
N2 supplement	1%	Thermo Fisher Scientific, A1370701
MEM non-essential amino acids solution	1%	Thermo Fisher Scientific, 11140050
Glutagro supplement	1%	Corning, 25-015-C1
Penstrep	1%	Thermo Fisher Scientific, 15140163
CHIR99021	0.01%	Tocris, 4423
DMH-1	0.01%	Tocris, 4126
SB431542	0.02%	Tocris, 1614
BMP4	0.2%	R&D systems, 314-BP-010/CF
Y-27632 2HCl (only on Day 0)	0.1%	Hello Bio, HB2297
All-trans retinoic acid (only on day 4 and 5)	0.01%	Sigma Aldrich, R2625

B. Complete Sphere Culture Medium

Ingredient	Final concentration	Supplier and Catalogue number
DMEM/F12	47%	Thermo Fisher Scientific, 21331020
Neurobasal	47%	Thermo Fisher Scientific, 21103049
B27 supplement	2%	Thermo Fisher Scientific, 17504044
N2 supplement	1%	Thermo Fisher Scientific, A1370701
MEM non-essential amino acids solution	1%	Thermo Fisher Scientific, 11140050
Glutagro supplement	1%	Corning, 25-015-C1
Penstrep	1%	Thermo Fisher Scientific, 15140163
CHIR99021	0.01%	Tocris, 4423
FGF2	0.1%	R & D systems, 233-FB-010/CF
Y-27632 2HCl	0.1%	Hello Bio, HB2297
All-trans retinoic acid (only on day 4 and 5)	0.01%	Sigma Aldrich, R2625

C. Complete ENS Culture Medium

Ingredient	Final concentration	Supplier and Catalogue number
BrainPhys Neuronal medium	92.5%	Thermo Fisher Scientific, 21331020
B27 supplement	2%	Thermo Fisher Scientific, 17504044
N2 supplement	1%	Thermo Fisher Scientific, A1370701
MEM non-essential amino acids solution	1%	Thermo Fisher Scientific, 11140050
Glutagro supplement	1%	Corning, 25-015-C1
Penstrep	1%	Thermo Fisher Scientific, 15140163
GDNF	0.1%	Peprotech, 450-10
DAPT	0.1%	Tocris, 2634
Ascorbic acid	0.3%	Sigma Aldrich, 113170-55-1
Vitronectin	1%	Thermo Fisher Scientific, A14700

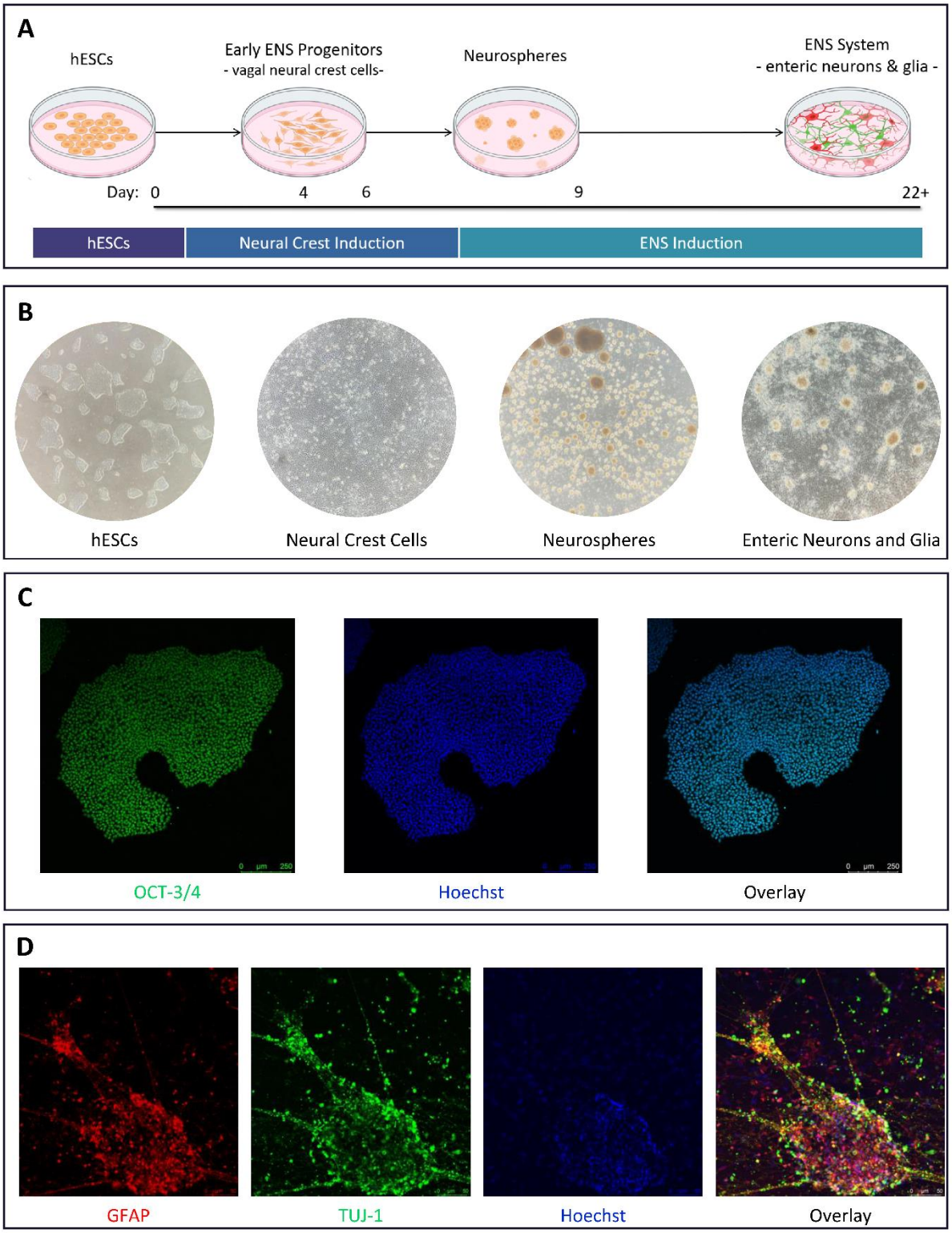

*Figure 1 – (**A**) Workflow for the generation of hESC-derived in vitro ENS cells (**B**) Representative brighfield images of cells in different stages of the differentiation protocol (**C**) Confocal images of hESCs used in the differentiation protocols, positive for OCT3/4 and Hoechst, and respective overlay (**D**) Confocal images of enteric neurons and enteric glial cells at the end of the differentiation; stained for GFAP, TUJ-1, and Hoechst, and respective overlay*

2.3 | Acute Pro-inflammatory Stimulation and Acetate Exposure

On day 30 of the differentiation protocol, the ENS cells were exposed to either an LPS (10µg/mL) or a pro-inflammatory cytokine mix (30ng/mL TNF-α and 10ng/mL IL-1β) enriched Complete ENS Culture Medium for 24 hours. The two chosen treatment conditions have been previously shown to induce inflammation in the ENS cells. To test the anti-inflammatory effect of acetate, sodium acetate (Sigma, S2889) was dissolved in cell culture water to obtain a 100mM stock solution. This was further filtered and sterilised using a syringe filter, and the appropriate quantity of the stock was added to the treatment conditions to test the effect of different final acetate concentrations (1mM, 5mM, 10mM). Following the 24-hour exposure, the cell medium was collected and stored at -20^{o}C for further experiments. Afterwards, a resazurin-based cell viability assay was performed, and then, cells were fixed using 4% paraformaldehyde in PBS at room temperature for 15 minutes and kept in PBS at 4^{o}C until immunocytochemistry was performed.

2.4 | Chronic Pro-inflammatory Stimulation

Two individual experiments were performed to test the effects of a long-term exposure to proinflammatory stimuli on the ENS cells (an overview of the experimental setup is described in Figure 2A&B). For the first trial experiment, the ENS cells were kept until day 33 of the differentiation protocol and further exposed to different concentrations of LPS (100ng/mL, 1µg/mL, 10µg/mL) or cytokine mix (5ng/mL TNF-α & 5ng/mL IL-1β, 10 ng/mL TNF-α & 10 ng/mL IL-1β, 30 ng/mL TNF-α & 10 ng/mL IL-1β) for 8 days. In the second experiment, the ENS cells were kept until day 26 of the differentiation protocol and further exposed to a combination of 5 ng/mL TNF-α and 5 ng/mL IL-1β for 14 days. In both experiments, full medium changes were performed every other day, and the culture medium supernatant was collected and stored at -20^{o}C for further experiments. Following the collection of the cell supernatant on the last days of the experiments, a resazurin-based cell viability assay was performed, and afterwards, cells were fixed using 4% paraformaldehyde in PBS at room temperature for 15 minutes and further kept in PBS at 4^{o}C until immunocytochemistry was performed.

2.5 | Resazurin Assay

The resazurin-based cell viability assay was performed to establish the cytotoxic effects of the treatments used in the performed experiments. After the completion of each experiment, the cells were incubated for 3h with 85uL/cm2 resazurin solution, diluted 1:10 in Complete ENS Culture Medium. Following the incubation, cell supernatants were transferred in a flat bottom 96-well plate (100µL/well), and absorbance intensity was measured at 560nm with a reference at 600nm. Further, the cell viability rate was assessed by evaluating the percentage of live, healthy cells in the treatment groups compared to the live, healthy cells in the control group, calculated by dividing the mean absorbance of treated cells by the mean absorbance of control cells.

2.6 | Immunocytochemical Staining

Immunocytochemical staining of OCT3/4 was done on hESCs, and staining of GFAP, TLR-4, α-syn, p-α-syn, and TUJ-1 was performed on ENS-generated cells fixed using 4% paraformaldehyde in PBS at room temperature for 15 minutes and kept in PBS at 4°C for up to 10 days. Cells were permeabilised in PBS containing 0.2% Triton-X 100 for 15 minutes, followed by two 5-minute washes with PBS. Blocking was done using blocking buffer (3%

BSA/3% NGS in PBS) for one and a half hours at room temperature, followed by overnight incubation, with the primary antibody (Table 2) diluted in blocking buffer. The overnight incubation was followed by three consecutive washes with PBS of 5 minutes each. The secondary antibody (Table 2) was diluted in freshly prepared blocking buffer and incubated in the dark for 2 hours at room temperature. For the counterstaining of DNA, the Hoechst Solution was used. Plates were kept in the dark at 4ºC until imaging was performed. Imaging was performed on a Leica TCS SP8 confocal microscope with a 63x oil immersion or a 25x water immersion lens.

Table 2 - List of primary and corresponding secondary antibodies used for immunocytochemistry

Primary Antibody	Secondary Antibody
Anti-OCT3/4 (1:200, sc-5279, Santa Cruz Biotechnology)	Goat anti-mouse 488 (1:500, A11001, ThermoFisher)
Anti-GFAP (1:1000; z0334; Dako)	Goat anti-rabbit 594 (1:500, A-11072, ThermoFisher)
Anti-TLR4 (1:500, 66350-1-Ig, Proteintech)	Goat anti-mouse 488 (1:500, A11001, ThermoFisher)
Anti-α-syn (1:100, 04-1053, Millipore)	Goat anti-rabbit 594 (1:500, A-11072, ThermoFisher)
Anti-p129-syn (1:500, Ab51253, abcam)	Goat anti-rabbit 594 (1:500, A-11072, ThermoFisher)
Anti-TUJ-1 (1:500, 801201, BioLegend)	Goat anti-mouse 488 (1:500, A11001, ThermoFisher)

2.7 | Enzyme-Linked Immunosorbent Assay

The collected culture medium supernatants from ENS-generated cells treated with different conditions were used to quantify the pro- and anti-inflammatory markers. The levels of Interleukin-6 (IL-6), Interleukin-4 (IL-4) and Interleukin-8 (IL-8) were assessed via an Enzyme-linked immunosorbent assay (ELISA) by using the Human IL-6 Uncoated ELISA Kit (88-7066-88, ThermoFisher), the IL-8 Human Uncoated ELISA Kit (88-8086-88, ThermoFisher), and the IL-4 Human Uncoated ELISA Kit (88-7046-88, ThermoFisher), which were used according to the manufacturer's instructions. Analysis of the ELISA data was done using GainData (Arigo Biolaboratories). The standard curve was plotted using 4-parameter logistic regression. Control samples were added undiluted, while medium samples were tested at either 10 or 100-fold dilutions, depending on the performed analysis for the readings to fit within the linear region of the standard curve. The generated standard curve was used to calculate the cytokines' concentrations in each sample.

2.8 | Statistical Analysis

Prism 9.0 GraphPad Software (GraphPad, San Diego, CA, USA) was used for statistical analysis. Statistical analysis was done by performing an ordinary one-way analysis of variance (ANOVA) for the cell viability assay and the acetate experiment. A mixed-effect analysis was performed for the chronic exposure treatments, evaluating the differences within the individual days and the changes within one treatment group over the course of the experiment. Differences were considered statistically significant when $p < 0.05$.

2.9| Metabolomics

2.9.1 | Extracellular Metabolomics

Preparation of the extracellular metabolomic components was done by collecting 10µL of the culture supernatant and lysing it with 1mL lysis buffer containing methanol:acetonitrile:dH2O (2:2:1). The samples were shaken for 10 minutes at 4°C and then centrifuged at 16.000g for 15

minutes at 4°C to remove cell debris and proteins. Further, the supernatant was used for LC-MS analysis.

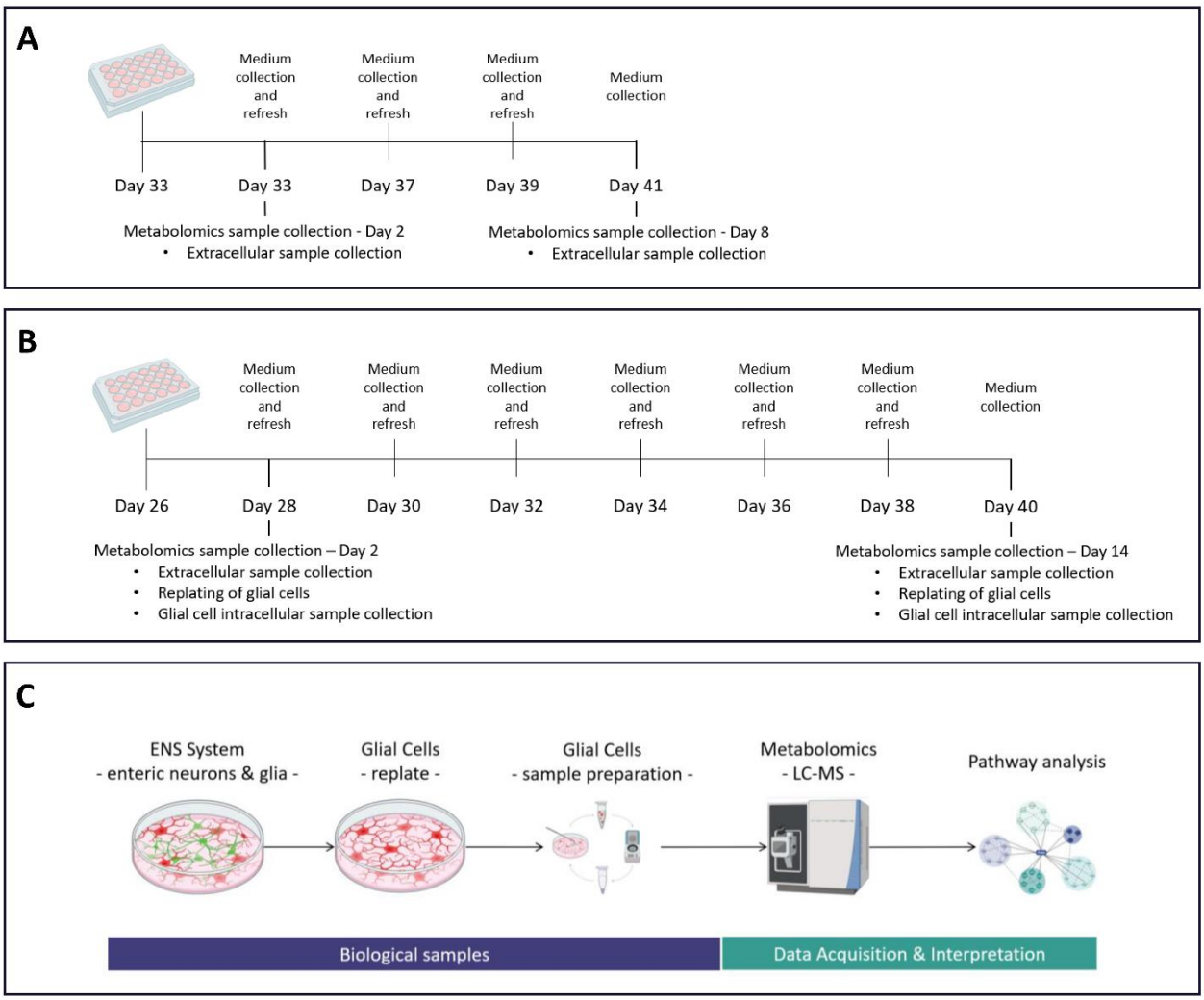

*Figure 2 – Experimental overview of workflow for (**A**) Chronic Pro-inflammatory Stimulation Trial and (**B**) Chronic Pro-inflammatory Stimulation Experiment. (**C**) Glial cell harvest and metabolomics workflow*

2.9.2 | Intracellular Metabolomics

For the analysis of the intracellular metabolism of EGCs, theco-cultured ENS cells were incubated with Accutase for 25 minutes at 37°C to allow the formation of single cells, followed by neutralisation using DMEM:F12. The single-cell suspension was centrifuged for 5 min at 300g. The supernatant was discharged, and the cells were resuspended in their original Complete ENS Culture Medium. The cells were replated onto newly coated Matrigel plates and incubated for 2h at 37°C. Following incubation, which allows the attachment of the EGCs only and their isolation, the cell culture supernatant was collected, and the attached EGCs were washed with ice-cold PBS. Extraction of intracellular metabolites was done with 500uL lysis buffer containing methanol:acetonitrile:dH_2O (2:2:1) while using a cell scraper. The samples were shaken for 10 minutes at 4°C and then centrifuged at 16.000g for 15 minutes at 4°C to remove cell debris and proteins. Further, the supernatant was used for LC-MS analysis.

2.9.3 | LC-MS Analysis

LC-MS analysis was performed on an Exactive mass spectrometer (Thermo Scientific) coupled to a Dionex Ultimate 3000 autosampler and pump (Thermo Scientific), for the extracellular samples or Q-Exactive HF mass spectrometer (Thermo Scientific) coupled to a Vanquish autosampler and pump (Thermo Scientific) for the intracellular samples. The MS operated in polarity-switching mode with spray voltages of 4.5 kV and -3.5 kV. Metabolites were separated using a Sequant ZIC-pHILIC column (2.1 x 150 mm, 5 µm, guard column 2.1 x 20 mm, 5 µm; Merck) with elution buffers acetonitrile (eluent A) and eluent B (20 mM $(NH_4)_2CO_3$, 0.1% NH_4OH in ULC/MS grade water (Biosolve)). Gradient ran from 20% eluent B to 60% eluent B in 20 minutes, followed by a wash step at 80% and equilibration at 20%. The flow rate was set at 150 µl/min. Analysis was performed using Tracefinder software (Thermo Scientific). Metabolites were identified and quantified based on exact mass within 5 ppm and further validated by concordance with retention times of standards. Peak intensities were normalised based on total ion count.

2.9.4 | Metabolomics Data Processing and Analysis

Raw data files acquired from the Tracefinder software were processed and analysed using RStudio Version: 2023.12.0+369. The processed data was used to perform the enrichment analysis using MetaboAnalyst 5.0.

3 | Results

3.1 | Acute Pro-inflammatory Stimulation and Acetate Exposure

The aim of this experiment was to investigate the effect of acetate on the inflammation induced by pro-inflammatory stimuli, either LPS or a cytokine mix, in the ENS cells. The ENS cells were exposed to LPS (10µg/mL) or a pro-inflammatory cytokine mix (30ng/mL TNF-α and 10ng/mL IL-1β) in combination with different concentrations of acetate (1mM, 5mM, and 10mM) for 24h. After the 24h exposure, cell culture supernatants were collected and subsequently tested via ELISA to check for the production of the pro-inflammatory cytokine IL-6. Exposure of the ENS cells to LPS induced a low release of IL-6, and no decrease in the level of IL-6 was noticed in any of the different conditions (Figure 3A). The exposure of the ENS cells to pro-inflammatory cytokines (TNF-α and IL-1β) induced a high release of IL-6 (Figure 3B). However, the addition of acetate failed to hamper the production of IL-6 following exposure to pro-inflammatory cytokines.

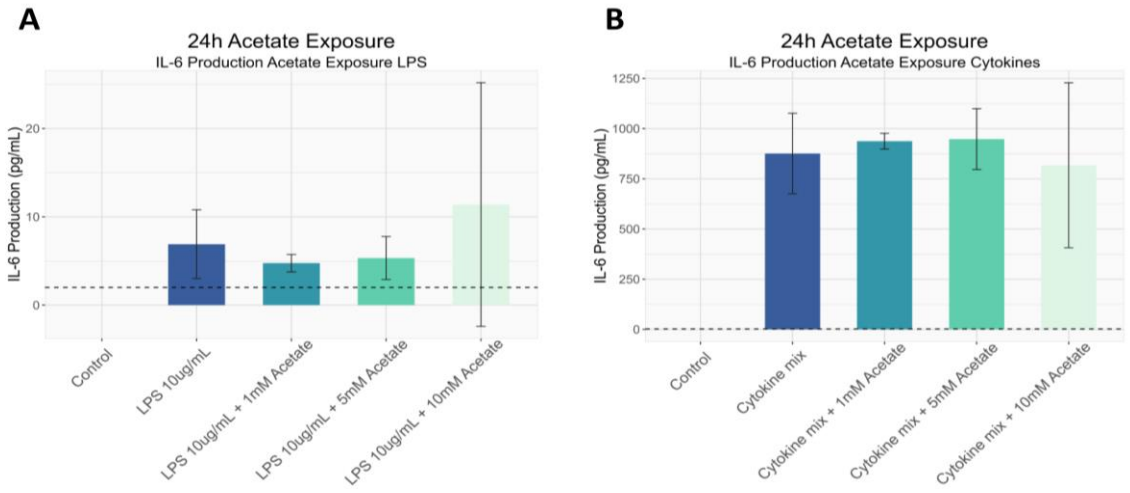

*Figure 3 – IL-6 cytokine production in culture medium supernatant measured 24h following the acetate experiment for (**A**) LPS-treated cells and (**B**) cytokine-treated cells. Dotted line represents the lower limit of detection of the used ELISA kit (2pg/mL); (mean+sd) n=3 per condition*

3.2 | Chronic Pro-inflammatory Stimulation | Trial

This experiment aimed to investigate the effect of long-term exposure to pro-inflammatory stimuli on the ENS cells. For this, the ENS cells were exposed to different concentrations of LPS (100ng/mL, 1µg/mL, 10µg/mL) or a pro-inflammatory cytokine mix (5ng/mL TNF-α & 5ng/mL IL-1β, 10 ng/mL TNF-α & 10 ng/mL IL-1β, 30 ng/mL TNF-α & 10 ng/mL IL-1β).

The cell viability assay analysis showed that the 8-day exposure to LPS did not induce cell death in the ENS cells (Figure 4A). Levels of IL-6 in the culture supernatant of the LPS-treated cells were under the lower limit of quantification (Figure 4B). Analysis of the cell viability assay for the 8-day exposure of the ENS system to the TNF-α and IL-1β mix did not induce cell death in our ENS cells (Figure 4C). During the 8-day exposure, full medium changes were performed every other day, during which cell culture supernatant was collected and further used to evaluate the levels of IL-6. In the culture supernatant of the cytokine-treated cells, an increase in the production levels of IL-6 in all three treatment conditions on day 2 is observed. However, over the course of the experiment, a progressive decrease in the levels of IL-6 in all treatment conditions is seen, suggesting an accommodation of the ENS cells to the pro-inflammatory environment (Figure 4D). The levels of IL-4 following 8-day exposure of the

ENS system to the IL-1β and TNF-α mix were also evaluated (data not shown). However, the values obtained were below the detection range of the used ELISA kit (2pg/mL), thus, this analysis was not pursued any further.

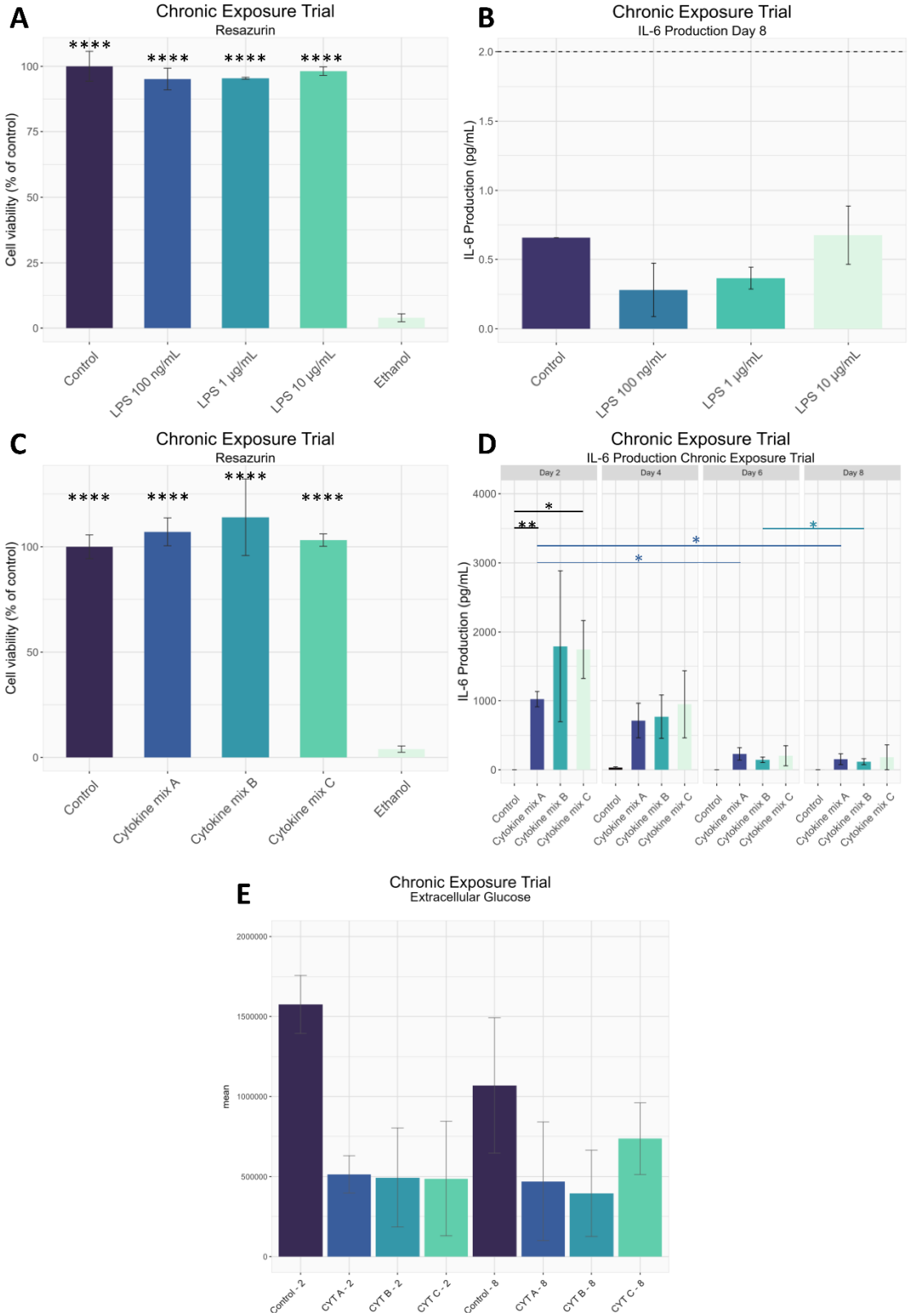

*Figure 4 – Result of the Chronic Pro-inflammatory Stimulation Trial – (**A**) Cell viability assay on day 8 and (**B**) IL-6 production in culture medium supernatant measured on day 8 for LPS-treated cells. Dotted line represents the lower limit of detection of the used ELISA kit (2pg/mL) (**C**) Cell viability assay on day 8, (**D**) IL-6 production in culture medium supernatant measured on days 2,4,6, and 8, and (**E**) extracellular glucose levels on days 2 and 8 for the cytokine-treated cells *P<0.05,**P<0.01,**** P<0.0001 (mean+sd) n=3 per condition*

Next, we analysed the differences in extracellular metabolites present in the ENS cell supernatant collected on day 2 and day 8. No notable differences were observed in the majority the studied metabolites. However, when studying the differences in glucose levels, we observe that the cytokine-treated cells take up more glucose than the respective controls throughout the experimental period (Figure 4E). These observations suggests that the cytokine treatment, regardless of the concentration, has a significant effect on the metabolic processes by increasing the rate of glucose uptake and promoting a metabolic shift towards glycolysis.

3.3 | Chronic Pro-inflammatory Stimulation

Prompted by the initial results of the chronic exposure treatment trial we performed, we aimed to redo the experiment with the intention of gathering more results that would help us understand the drivers of accommodation of the ENS system to the pro-inflammatory environment. Moreover, we aimed to evaluate the general effect of proinflammatory cytokines over a longer period of time and look for signs of aggregated α-synuclein, which was not observed in our initial experiment. For this, the chronic inflammation was simulated by exposing the cells to a mix of 5ng/mL TNF-α & 5ng/mL IL-1β over the course of 14 days. After the 14-day exposure to the combination of the pro-inflammatory cytokines, cell culture supernatants collected through the experimental period were tested via ELISA for IL-6 and IL-8. Similarly to our initial trial, similar trends in the expression levels of IL-6 in the culture supernatant can be observed. Levels of IL-6 increase in the first 48h following exposure and decrease over the course of the following days, remaining at constant values from day 6 up to day 14 (Figure 5B). When looking at the expression levels of IL-8, a similar trend as with the release of IL-6 is seen, on day 2, observing a high release of IL-8 and then a decrease in the following days. However, unlike with the release of IL-6, throughout the course of the experimental period, same drop in the release of IL-8 is not observed (Figure 5C).

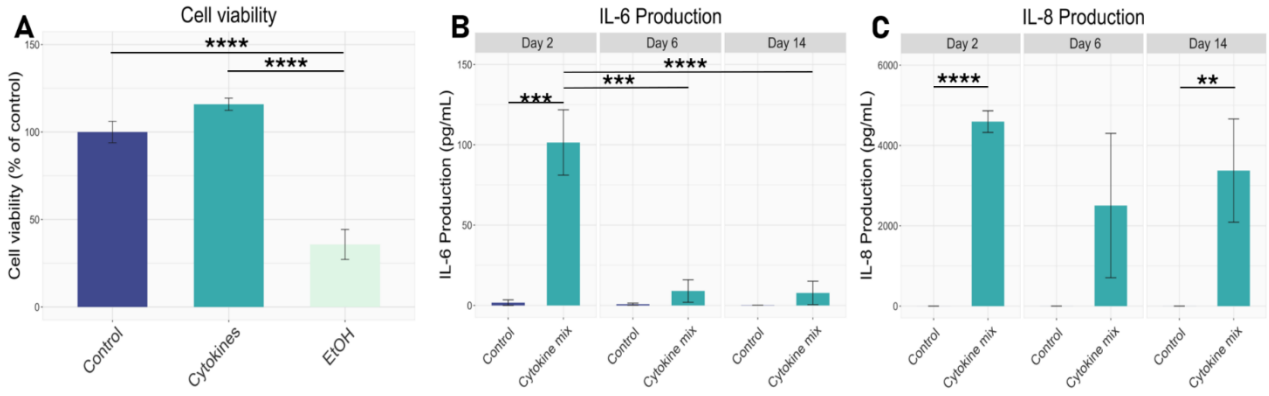

*Figure 5 – Result of the Chronic Pro-inflammatory Stimulation Experiment – (**A**) Cell viability assay on day 14 and pro-inflammatory cytokine production in culture medium supernatant measured on days 2, 6 and 14 of the experiment (**B**) IL-6 and (**C**) IL-8 **P<0.01, ***P<0.001, **** P<0.0001 (mean+sd) n=6 per condition*

To assess the effects of the chronic exposure of pro-inflammatory cytokines on the formation of α-syn aggregates, immunocytochemical staining (section 2.6) for α-syn and p129syn was performed. When looking at the α-syn staining no notable differences between the control and cytokine treated cells can be observed, both samples expressing α-syn (Figure 6A). However, when looking at the phosphorylated α-syn, preliminary observations show that in the cytokine treated cells, p129syn is being expressed in the soma of the neurons (Figure 6B). These observations are preliminary, and no statistical analysis was conducted since not enough

regions of interest were identified. However, these observations could have an important role in establishing the factors responsible for the formation of alpha-synuclein aggregates.

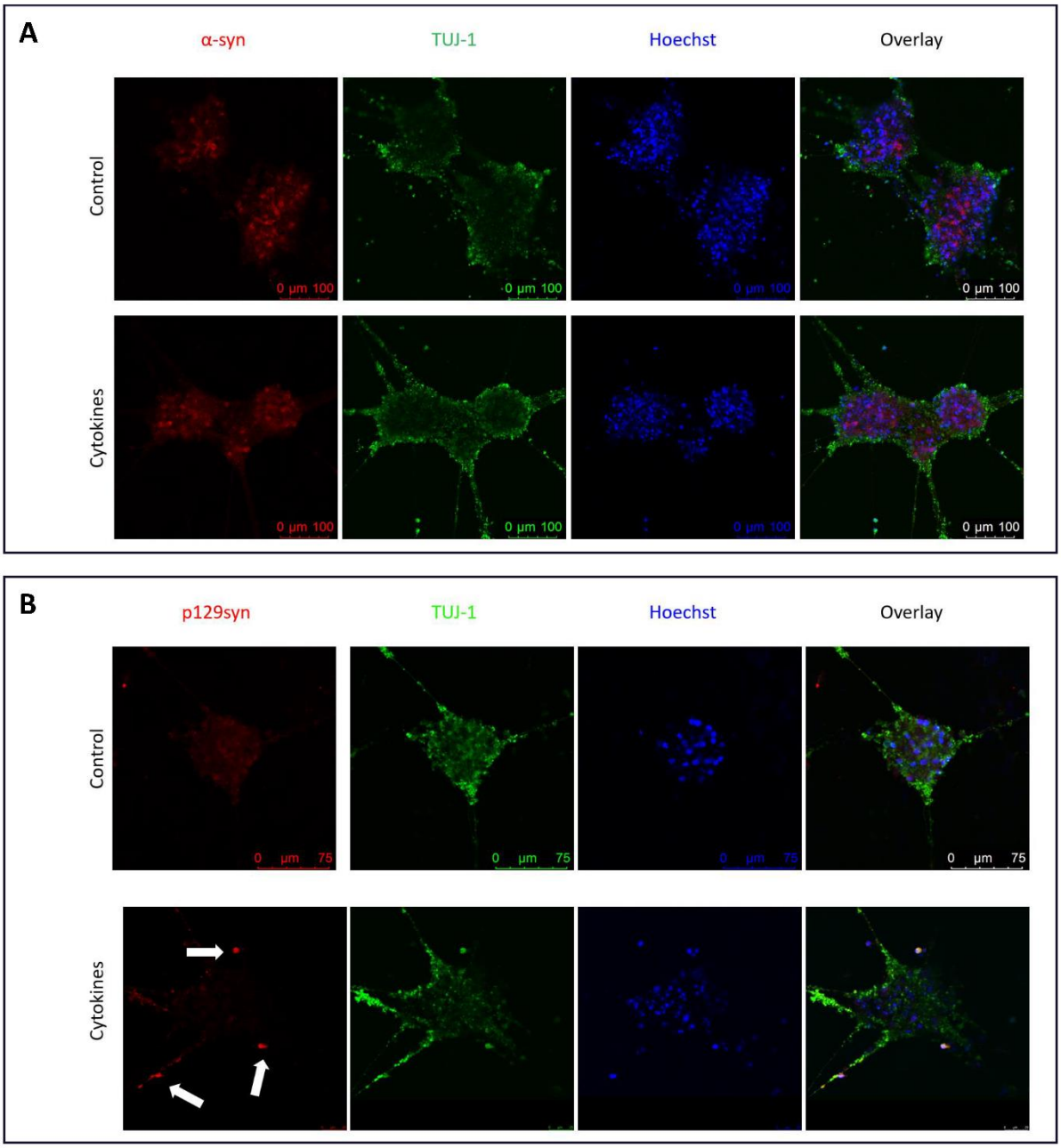

*Figure 6 - Confocal images of ENS cells following the Chronic Pro-inflammatory Stimulation Experiment – Expression of (**A**) a-syn and (**B**) p129syn in (top) control and (bottom) cytokine treated cells. Both control and cytokine-treated cells express a-syn; however signs of p129syn were present only in the soma of neurons of the cytokine-treated ENS cells (white arrows).*

Next, the differences in extracellular metabolites present in the ENS cell supernatant collected on day 2 and day 14 were analysed. No notable differences were noted in most of the studied metabolites. However, just like in the initial trial, when studying the differences in glucose levels, it is observed that the cytokine-treated cells take up more glucose than the respective controls throughout the experimental period (Figure 7A). At the same time we observe that on day 2 the cytokine treated cells show higher levels on extracellular lactate, however, the same trend cannot be said for the cells on day 14 (Figure 7B). Taken together, the decreased levels

of glucose and increased levels of lactate observed in the control cells, reveal that the cytokine treatment has an important impact on metabolic processes by promoting a metabolic shift towards glycolysis.

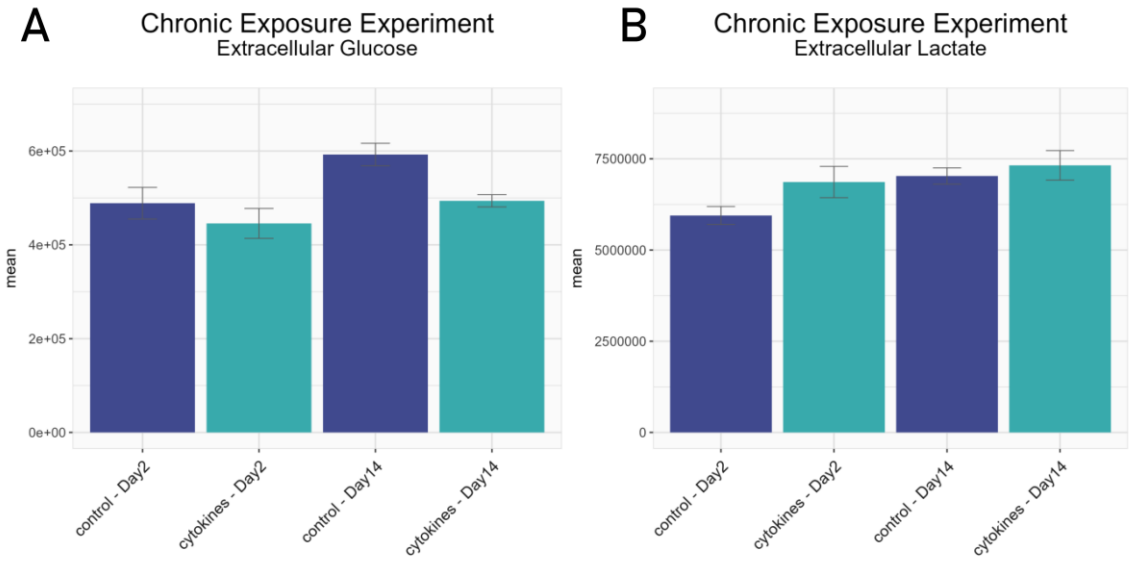

*Figure 7 – Result of the Chronic Pro-inflammatory Stimulation Experiment - Extracellular levels of (**A**) glucose and (**B**) lactate levels on days 2 and 14 in the culture medium supernatant in the cytokine-treated cells.*

Further, an evaluation of the intracellular metabolic changes of EGCs was performed on day 2 and day 14 of the chronic exposure treatment in order to establish the changes in energy production and immune response. To assess metabolic differences between control and cytokine treated EGCs, cells were lysed for metabolite extraction and used for subsequent analysis. The PCA plot shows the overall differences in the expression levels of all intracellular metabolites and was used to visualize the clustering of samples belonging to the different groups (Figure 8A). On day 2 the cytokine treated cells show no difference in metabolic phenotype compared to the respective controls since they overlap in the PCA. However, on day 14, the cytokine treated cells show a complete different metabolic phenotype than the respective controls. To determine the specific metabolic pathways that were altered, a metabolite enrichment analysis was performed with MetaboAnalyst 5.0. Based on the ranking of metabolites according to their impact on the metabolic pathways major enrichments in various pathways between the cytokine-treated cells and respective controls on day 14 can be observed. Multiple pathways involved in energy production (alanine, aspartate and glutamate metabolism, lysine degradation, citrate cycle (TCA cycle), galactose metabolism, pyruvate metabolism, glycolysis/gluconeogenesis), oxidative stress (glutathione metabolism, arginine biosynthesis, alanine, aspartate and glutamate metabolism), nucleotide synthesis (pyrimidine metabolism, aminoacyl-tRNA biosynthesis, purine metabolism), and pathways providing adequate immune effector response (glycolysis, pentose phosphate pathway, fatty acid degradation, amino acid metabolism, TCA cycle) are altered between day 2 and day 14.

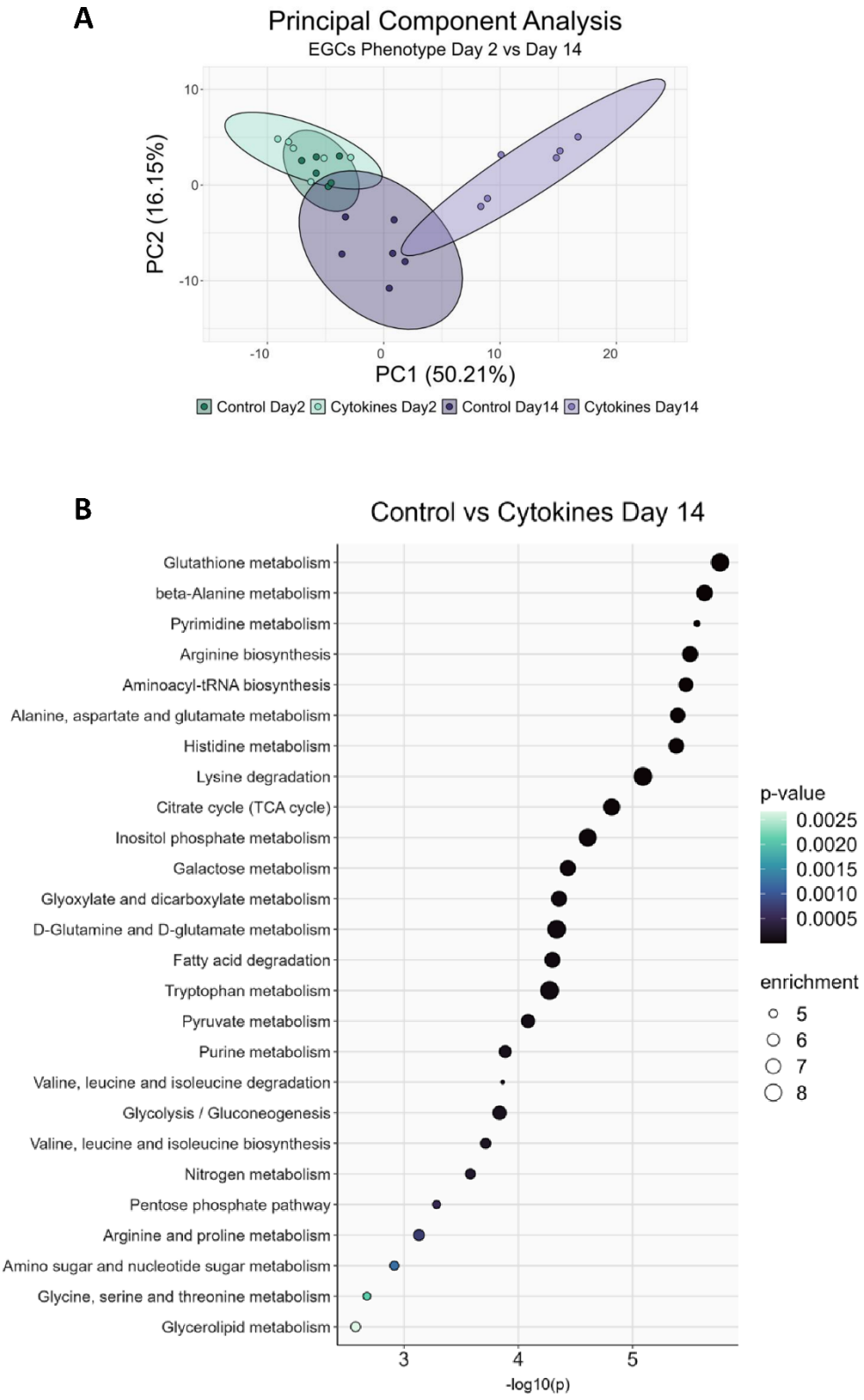

*Figure 8 – Intracellular metabolomics results for the Chronic Pro-inflammatory Stimulation Experiment. (**A**) PCA plot of metabolomics profile from mean intensity values of total detected metabolites. (**B**) Overview of pathway analysis depicting enrichment ratio in order of statistical significance.*

Lastly, a detailed analysis of all the intracellular metabolites that were identified during the experiment was performed. Our main objective was to observe the modification in the expression of intracellular metabolites between day 2 and day 14 by analyzing the fold change of these metabolites. The plot of this analysis can be seen in Figure 9. Identified metabolites have been color-coded based on the metabolic pathway they are mostly involved in, however, no clear trends based on specific metabolic pathways have been identified.

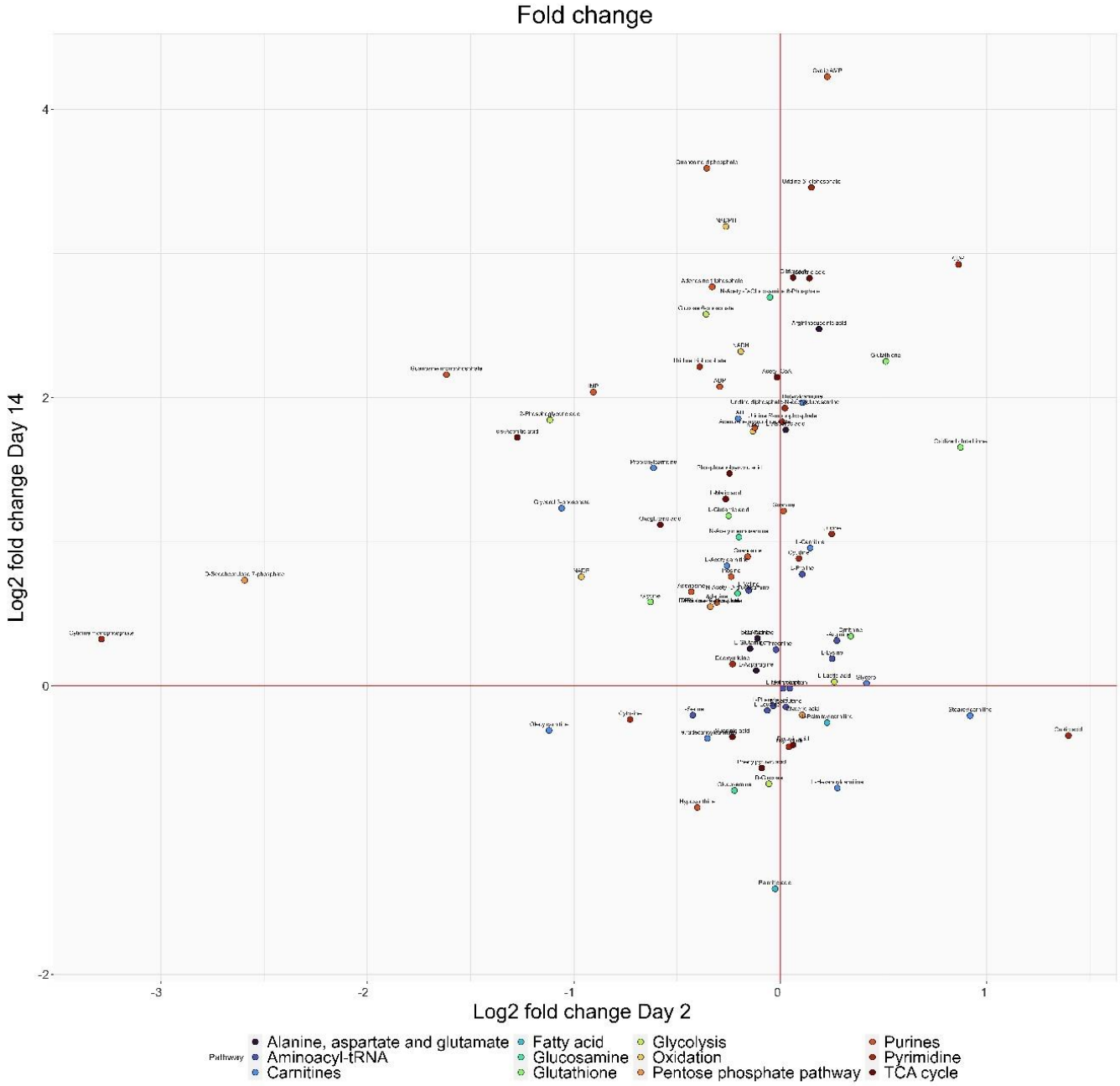

Figure 9 – Fold change of metabolites present in our analysis, color coded based on the metabolic pathways.

4 | Discussion

4.1 | Acute Pro-inflammatory Stimulation and Acetate Exposure

In the present trial experiment, the expression levels of IL-6 in the cell culture supernatant following a 24-hour incubation of the ENS model with pro-inflammatory stimuli in combination with different acetate concentrations was studied. Overall, no suppression of the inflammation was seen with any of the acetate concentrations in either LPS or cytokine-treated cells.

The pro-inflammatory effects of LPS are caused by the binding of this compound to the TLR4 (26). Following the experiment, immunocytochemistry was performed, and the TLR4 was not detected on the surface of the EGCs generated from this differentiation. Prior immunocytochemical staining sperformed on previous ENS cells generated by following the same differentiation protocol showed the expression of the receptor on the surface level of the EGCs. The lack of the TLR4 on the cell surface suggests that the cells generated in this differentiation lacked the conditions for fully develop and maturate within the same amount of time. Keeping the cells in culture for a longer time, though proven difficult due to the detaching of the neurospheres, would possibly allow for the maturation of the cells. A longer culture period could ensure proper expression of the TLR4 on the surface of the EGCs and the observation of an immune response in the ENS system following stimulation with LPS. Throughout the differentiation process, we encountered challenges with the detachment of the neurospheres, resulting in difficulties with cell culture. In order to maintain consistency among the iterations, day 30 was selected as the initial point for this experiment as well. While extending the culture time could have allowed full maturation of the cells and ensured the presence of the TLR4 receptor on their surface, it would also have posed a risk of sample loss, resulting in insufficient samples to perform the experiment.

For the cytokine-treated cells, we observed a high release of IL-6 in the culture supernatant following exposure to the pro-inflammatory stimuli; however, no suppression of the inflammation was noticed with any of the acetate concentrations. These results indicate that the chosen acetate concentrations were not high enough to suppress the inflammation caused by the pro-inflammatory cytokine mix. We know from previous studies that were performed in our group that 2mM of butyrate is enough to suppress the inflammation. Taking into account the approximate ratio of SCFAs present in the gut (acetate:butyrate ≈ 30:2) (27), we can hypothesise that a concentration of minimum 30mM of acetate might be more effective in inducing anti-inflammatory effects. Repeating this experiment with higher acetate concentrations could help us validate this hypothesis and would further our understanding of the mechanism through which SCFAs suppress inflammation.

4.2 | Chronic Pro-inflammatory Stimulation | Trial

In this trial experiment, we studied the expression levels of IL-6 in the cell supernatant of the ENS model in response to long-term exposure to proinflammatory stimuli. We started by analysing the cell viability at the end of the chronic exposure to test that the treatment did not induce any cell death throughout the experiment. We see that for both LPS and cytokine mix treated cells, there are no signs of cytotoxicity at the end of the 8-day exposure period.

When looking at the production of IL-6 in the culture supernatant of the cells exposed to LPS, we see that the production of IL-6 is under detection levels on day 8. Following the experiment,

immunocytochemistry was performed, and the TLR4 receptor was not detected in the EGCs generated for this experiment. The cells from this experiment and those used for the acute pro-inflammatory stimulation and acetate exposure experiment were generated at the same time, during the same differentiation; however, the acute pro-inflammatory stimulation and acetate exposure experiment was performed 3 days before the start of the chronic pro-inflammatory stimulation experiment. Therefore, despite not seeing the TLR4 expressed on the EGCs in the acetate experiment, we expected that the cells in this experiment, by being cultured for an additional 10 days, would express the receptor by the end of the experimental period. Despite the additional culture time, allowing for the cells to mature, the TLR4 could not be identified on the cell surface of the ENS cells by the end of the experiment (day 41 of the differentiation protocol). To test the effects of a long-term exposure with LPS on the ENS model, we need to validate on which day of the differentiation the EGCs are mature enough and express the TLR4.

When looking at the effects of the prolonged exposure of the ENS cells to pro-inflammatory cytokines, we see an increase in the release of IL-6 on day 2 of the exposure and a steady decrease over the course of the 8-day experiment. We know that short term exposure of pro-inflammatory stimuli induces phenotypic changes of EGCs, shift them towards an anti-inflammatory profile, resulting in neuroprotective effects. However, chronic exposure to proinflammatory cytokines could induce enteric glia to enter reactive gliosis, therefore potentially contributing to the pro-inflammatory environment. From our results, we cannot conclude that the EGCs enter reactive gliosis since the levels of the IL-6 steadily decrease over the course of the 8-day experiment. In order to establish this, in future experiments, we could look at the morphological changes of EGCs, measure the change in expression levels of glial markers (GFAP), and assess other inflammatory mediators or markers of gliosis (28–30). It is unclear through which mechanisms EGCs exercise their anti-inflammatory effects. Therefore, we aimed to study this further while also evaluating the intracellular metabolism of EGCs.

By looking at the levels of the extracellular metabolites in the co-culture cell supernatant, we see that cytokine-treated cells take up more glucose than control cells on day 2 and day 8. The increase in glucose uptake of EGCs suggests an increase in energy consumption, indicating high energetic demand, due to the activation of EGCs, which are acting to suppress the inflammation. This suggests that the cells become glycolytic on day 2 and remain in this state through the experimental period.

However, unlike with the results of IL-6, we do not see an accommodation to the pro-inflammatory state in terms of the cells' metabolism since, on day 8, we still observe a higher glucose uptake by the cytokine-treaded cells. The changes observed in the extracellular metabolites prompted us to further investigate the intracellular metabolism of EGCs in hopes of figuring out the mechanisms through which EGCs regulate ENS inflammation. Interestingly, this finding is contrary to the observed IL-6 production, where we see an accommodation of the cells to the pro-inflammatory environment.

Chronic exposure of pro-inflammatory cytokine to the ENS cells causes a high release of IL-6 on day 2 of the exposure and a steady decrease over the course of the 8-day experiment. When looking at uptake of glucose by the ENS cells, we observe that throughout the experiment, the cytokine-treated cells take up more glucose than the respective controls. The data suggests that the cytokine treatment has an important impact on cell metabolism, leading to increased glucose uptake and a shift towards glycolysis. This metabolic shift may have implications for

the overall function of the ENS cells, and further investigation is required to fully understand its impact.

3.3 | Chronic Pro-inflammatory Stimulation

In this experiment, we looked at signs of immune activation, by assessing the levels of IL-6 and IL-8 in the cell supernatant of the ENS cells in response to long-term exposure to proinflammatory cytokines. We started by testing the cell viability at the end of the chronic exposure to test the treatment did not induce any cell death throughout the 14-days of exposure.

When looking at the production of IL-6 in the culture supernatant of the cells exposed to the combination of 5 ng/mL TNF-α and 5 ng/mL IL-1β, we observe the same trend as in the first iteration of this experiment. We observe an increase in the release of IL-6 on day 2 of the exposure and a steady decrease over the course of the 14-day experiment. The steady decrease over the course of the experiment suggests a potential accommodation of the ENS cells to the chronic pro-inflammatory stimulation. The observed accommodation may be intricately linked to changes in the phenotype of EGCs, as the increase in IL-6 production aligned with the activation of the cells in response to the proinflammatory environment induced by the addition of TNF-α and IL-1β. Metabolic changes may occur as a result of the pro-inflammatory stimulation, contributing to the accommodation of the ENS cells to the chronic inflammation. Phenotypic changes of the EGCs may prompt the release of anti-inflammatory mediators or neurotrophic factors, creating an environment that promotes inflammation resolution and allows ENS cells to adapt to chronic pro-inflammatory stimulation.

When investigating the production of IL-8, we see a similar trend as with the IL-6 production. We observed a high release of IL-8 in the culture supernatant collected on day 2. Throughout the experiment, though not significant, we see a small decrease in IL-8 production. Again, this suggests that an accommodation of the cells to the pro-inflammatory environment could stem from the change in phenotype of the EGCs. IL-8 is a powerful chemoattractant and activator of neutrophils, which in turn allow the resolution of inflammation, repair, and a return to normal tissue function. Since the *in vitro* model used in these experiments is limited to cells of the ENS, therefore, missing other immune components present in the gut it is possible that in order to observe a full resolution of the inflammation in our model, we would need a more complex cell system. However, it is important to acknowledge that a more complex cell system, including immune and epithelial cells, will also alter the observed production of IL-6 following chronic exposure to pro-inflammatory cytokines. The complex crosstalk between the different cell populations is likely to shape the overall inflammatory response by release of additional signalling molecules, therefore altering the effects of the pro-inflammatory stimuli on the ENS cells.

IL-4 and IL-10 are the two most commonly studied anti-inflammatory cytokines in EGCs in the context of suppressing inflammation. We have previously studied the production of IL-4 in the ENS cell culture supernatant in the Acute Pro-inflammatory Stimulation and Acetate Exposure experiment; however, the measured IL-4 concentrations were under the detection limit; therefore, we can conclude that our ENS cells do not secrete IL-4 following the chronic exposure to pro-inflammatory cytokines. The absence of IL-4 in the cell supernatant implies that IL-4 is not actively involved in the context of inflammation and during the accommodation phase. This observation provides insight into the regulatory pathways involved in the complex and dynamic immunological processes within our experimental system. It would be valuable

to look at the levels of IL-10 in the culture supernatant in order to study the anti-inflammatory pathways that could be altered in the ENS cells, which in turn could be correlated to the phenotypic changes we observe by studying the metabolism of the EGCs.

In the first iteration of this experiment, we studied the expression of α-syn and could not observe α-syn in our cells. Prompted by these initial results, we redid this analysis in this experiment, this time also studying possible differences in the expression of p129syn. Preliminary analysis of the immunocytochemical staining shows p129syn present in the soma of neurons in the cytokine-treated cells but could not be observed in the controls. These preliminary results could play a significant role in establishing the reason for the formation of α-syn aggregates and establishing the pathogenic impact of α-synuclein phosphorylation. The phosphorylation of α-syn at Ser129 has been found to have major implications in regulating α-syn aggregation and neurotoxicity. The analysis of our samples was proven difficult due to the cell system detaching from the wells. Despite careful handling of the cells before and during the immunocytochemical staining process, the conditions were suboptimal, making it difficult to fully evaluate the expression of p129syn in the cells. Moreover, imaging was proven difficult, since the plates used in this experiment were not compatible for imaging the cells at a high magnification (63x), making it difficult to fully evaluate the cellular localization of p129syn. Considering that the detaching of the cells has been a major setback in all of the performed experiments, in the context of establishing the expression levels and cellular localisation of the p129syn, an alternative qualification method could be used. Such methods include SDS-PAGE, western blotting, flow cytometry, immunoassays (ELISAs or antibody array), or MS. Some of the mentioned techniques could also allow easy quantification of the p129syn, but they all present the disadvantage of not permitting the identification of the cellular localization of the protein of interest, which is an important factor in determining the pathogenic impact of α-synuclein phosphorylation.

In this study, we also analyzed the intracellular changes in EGC metabolism. The principal component analysis (PCA) shows a significant change in the metabolic phenotype between the cytokine-treated cells and controls on day 14. The difference in the metabolic phenotype observed in the PCA plot were in line with the differences observed in the pathway analysis. The analysis of the pathways in response to the two treatments revealed significant differences between them. As observed in the first trial (see section 3.2), the glycolysis pathway showed a significant difference, indicating an increase in energy production. This could be attributed to the EGCs' ability to respond to pro-inflammatory stimuli and balance the metabolic demand induced by inflammation. Additionally, the alanine, aspartate and glutamate metabolism, lysine degradation, galactose metabolism and pyruvate metabolism pathways are all pathways that could provide precursors to the TCA cycle, which further supports the increase in energy production. Furthermore, we also observed significant differences with pathways involved in the production of nitric oxide (NO). Glutathione metabolism, arginine biosynthesis as well as alanine, aspartate and glutamate metabolism are all involved in the production of NO activation of inducible nitric oxide synthase, a protein that catalyzes the production of NO. Nitric oxide is produced during inflammation and can contribute to oxidative stress, which in turn leads to damage to the enteric nervous system but also to the gut epithelial wall. In future experiments, measurements of the levels of oxidative stress in the ENS cells could be performed to fully understand the effects of exposure to chronic pro-inflammatory stimuli. It is important to note that nitric oxide is a crucial neurotransmitter involved in the intricate communication between

neurons within the ENS. It modulates smooth muscle contraction, regulates blood flow to the gastrointestinal tissue, and participates in neuroimmune interactions within the gut. The dual role of NO as both a contributor to inflammation and as a neurotransmitter highlights the significance of exploring the underlying pathways involved in its production. Moreover, we also identify pathways involved in the synthesis of nucleotides. These pathways include pyrimidine metabolism, aminoacyl-tRNA biosynthesis, and purine metabolism. Taken together, the significant differences observed with these metabolic pathways indicate the possible proliferation of EGCs during the exposure period. Lastly, we are also able to observe significant differences in metabolic pathways involved in providing adequate immune effector response. Such pathways involve glycolysis, the pentose phosphate pathway, fatty acid degradation, amino acid metabolism and the TCA cycle.

Lastly, we carried out a detailed analysis of all the intracellular metabolites that were identified during the experiment. Our main objective was to observe the modification in the expression of intracellular metabolites between day 2 and day 14 by analyzing the fold change of these metabolites. For this experiment, the purpose of this analysis was to gain a better understanding of how the metabolites change between day 2 and day 14 and to identify common trends in the production of metabolites and identify any notabledifferences between the two time points. In future experiments, this analysis could allow us to identify specific metabolites that have a common trends between days 2 and day 14, focusing on those showing the same trends on both days.

Our results show significant changes in multiple pathways, therefore, it is important to consider the overall changes in the metabolism of EGCs and its potential implications. A thorough examination of how metabolites are being altered is crucial to understanding the impact of the chronic exposure to pro-inflammatory cytokines. Additionally, it is important to investigate common pathways that play a role in blocking inflammation and study the trends of the metabolites implicated in these pathways.

By understanding the immuno-metabolic responses of EGCs to pro-inflammatory stimuli we can bridge the knowledge gap on the role of EGCs in inflammation. Not only can this shed light cellular mechanisms involved in the accommodation and resolution of inflammation but it can also open up new avenues for research into potential therapeutic targets for gut inflammation. Our research can therefore contributing to the understanding of early Parkinson's disease pathogenesis and progression, and contribute to the development of potential therapeutic targets for neurodegenerative disorders.

5 | Conclusion

This study aimed to investigate the immune-metabolic effects of (i) acetate on the inflammation induced by pro-inflammatory stimuli, either LPS or a cytokine mix, and (ii) long-term exposure to pro-inflammatory stimuli on an *in vitro* ENS model. The exposure to LPS failed to induce IL-6 release in both acute and chronic exposure experiments. Further investigations showed that the TLR4 was not present on the surface of EGCs. The acute pro-inflammatory cytokine stimulation in combination with acetate failed to suppress inflammation, suggesting that higher acetate concentrations are required to test the effects of acetate on the inflammation. Chronic pro-inflammatory cytokine stimulation of the ENS cells induced an increase in IL-6 production levels on day 2, which decreased progressively over time, suggesting an accommodation of the ENS cells to the pro-inflammatory environment. Moreover, significant changes in metabolic pathways in response to pro-inflammatory cytokines were observed. The results suggest a potential link between the adaptability of EGCs to the pro-inflammatory environment by modulating their metabolic activity. Further experiments are required to draw a definitive conclusions about EGCs' accommodation to chronic inflammation and the metabolic shifts that follow afterwards. Our research emphasizes the importance of studying the internal cellular mechanisms that control the response of EGCs to long-term inflammation. The main objective of these experiments was to examine the effects of chronic exposure to proinflammatory stimuli on the ENS cells. These preliminary observations could be used for the development of potential therapeutic targets for gut inflammation as well as for understanding early PD pathogenesis and progression.

References

1. Emin D, Zhang YP, Lobanova E, Miller A, Li X, Xia Z, et al. Small soluble α-synuclein aggregates are the toxic species in Parkinson's disease. Nat Commun. 2022 Sep 20;13(1):5512.
2. Zhu B, Yin D, Zhao H, Zhang L. The immunology of Parkinson's disease. Semin Immunopathol. 2022 Sep 8;44(5):659–72.
3. Warner TT, Schapira AH V. Genetic and environmental factors in the cause of Parkinson's disease. Ann Neurol. 2003;53(S3):S16–25.
4. Srinivasan E, Chandrasekhar G, Chandrasekar P, Anbarasu K, Vickram AS, Karunakaran R, et al. Alpha-Synuclein Aggregation in Parkinson's Disease. Front Med (Lausanne). 2021;8:736978.
5. Lee HM, Koh SB. Many Faces of Parkinson's Disease: Non-Motor Symptoms of Parkinson's Disease. J Mov Disord. 2015 May 31;8(2):92–7.
6. Goldman JG, Postuma R. Premotor and nonmotor features of Parkinson's disease. Curr Opin Neurol. 2014 Aug;27(4):434–41.
7. Chen QQ, Haikal C, Li W, Li MT, Wang ZY, Li JY. Age-dependent alpha-synuclein accumulation and aggregation in the colon of a transgenic mouse model of Parkinson's disease. Transl Neurodegener. 2018;7:13.
8. Tenreiro S, Eckermann K, Outeiro TF. Protein phosphorylation in neurodegeneration: friend or foe? Front Mol Neurosci. 2014 May 13;7.
9. Kawahata I, Finkelstein DI, Fukunaga K. Pathogenic Impact of α-Synuclein Phosphorylation and Its Kinases in α-Synucleinopathies. Int J Mol Sci. 2022 Jun 1;23(11):6216.
10. Jenner P. Oxidative stress in Parkinson's disease. Ann Neurol. 2003;53(S3):S26–38.
11. Van Den Berge N, Ferreira N, Gram H, Mikkelsen TW, Alstrup AKO, Casadei N, et al. Evidence for bidirectional and trans-synaptic parasympathetic and sympathetic propagation of alpha-synuclein in rats. Acta Neuropathol. 2019 Oct 26;138(4):535–50.
12. Kim S, Kwon SH, Kam TI, Panicker N, Karuppagounder SS, Lee S, et al. Transneuronal Propagation of Pathologic α-Synuclein from the Gut to the Brain Models Parkinson's Disease. Neuron. 2019 Aug;103(4):627-641.e7.
13. Kelly LP, Carvey PM, Keshavarzian A, Shannon KM, Shaikh M, Bakay RAE, et al. Progression of intestinal permeability changes and alpha-synuclein expression in a mouse model of Parkinson's disease. Movement Disorders. 2014 Jul 4;29(8):999–1009.
14. Carabotti M, Scirocco A, Maselli MA, Severi C. The gut-brain axis: interactions between enteric microbiota, central and enteric nervous systems. Ann Gastroenterol. 2015;28(2):203–9.
15. Metzdorf J, Tönges L. Short-chain fatty acids in the context of Parkinson's disease. Neural Regen Res. 2021;16(10):2015.

16. Hasan N, Yang H. Factors affecting the composition of the gut microbiota, and its modulation. PeerJ. 2019 Aug 16;7:e7502.

17. Di Vincenzo F, Del Gaudio A, Petito V, Lopetuso LR, Scaldaferri F. Gut microbiota, intestinal permeability, and systemic inflammation: a narrative review. Intern Emerg Med. 2023 Jul 28;

18. Mou Y, Du Y, Zhou L, Yue J, Hu X, Liu Y, et al. Gut Microbiota Interact With the Brain Through Systemic Chronic Inflammation: Implications on Neuroinflammation, Neurodegeneration, and Aging. Front Immunol. 2022 Apr 7;13.

19. Benvenuti L, D'Antongiovanni V, Pellegrini C, Antonioli L, Bernardini N, Blandizzi C, et al. Enteric Glia at the Crossroads between Intestinal Immune System and Epithelial Barrier: Implications for Parkinson Disease. Int J Mol Sci. 2020 Dec 2;21(23):9199.

20. Schneider S, Wright CM, Heuckeroth RO. Unexpected Roles for the Second Brain: Enteric Nervous System as Master Regulator of Bowel Function. Annu Rev Physiol [Internet]. 2019 Feb 10;81(1):235–59. Available from: https://doi.org/10.1146/annurev-physiol-021317-121515

21. Progatzky F, Pachnis V. The role of enteric glia in intestinal immunity. Curr Opin Immunol. 2022 Aug;77:102183.

22. Afridi R, Kim JH, Rahman MH, Suk K. Metabolic Regulation of Glial Phenotypes: Implications in Neuron–Glia Interactions and Neurological Disorders. Front Cell Neurosci. 2020 Feb 11;14.

23. Vinolo MAR, Rodrigues HG, Nachbar RT, Curi R. Regulation of Inflammation by Short Chain Fatty Acids. Nutrients. 2011 Oct 14;3(10):858–76.

24. Unger MM, Spiegel J, Dillmann KU, Grundmann D, Philippeit H, Bürmann J, et al. Short chain fatty acids and gut microbiota differ between patients with Parkinson's disease and age-matched controls. Parkinsonism Relat Disord. 2016 Nov;32:66–72.

25. Gogolou A, Frith TJR, Tsakiridis A. Generating Enteric Nervous System Progenitors from Human Pluripotent Stem Cells. Curr Protoc. 2021 Jun 8;1(6).

26. Lu YC, Yeh WC, Ohashi PS. LPS/TLR4 signal transduction pathway. Cytokine. 2008 May;42(2):145–51.

27. Yang LL, Millischer V, Rodin S, MacFabe DF, Villaescusa JC, Lavebratt C. Enteric short-chain fatty acids promote proliferation of human neural progenitor cells. J Neurochem. 2020 Sep 18;154(6):635–46.

28. Pochard C, Coquenlorge S, Freyssinet M, Naveilhan P, Bourreille A, Neunlist M, et al. The multiple faces of inflammatory enteric glial cells: is Crohn's disease a gliopathy? American Journal of Physiology-Gastrointestinal and Liver Physiology. 2018 Jul 1;315(1):G1–11.

29. von Boyen GBT. Proinflammatory cytokines increase glial fibrillary acidic protein expression in enteric glia. Gut. 2004 Feb 1;53(2):222–8.

30. Schneider R, Leven P, Mallesh S, Breßer M, Schneider L, Mazzotta E, et al. IL-1-dependent enteric gliosis guides intestinal inflammation and dysmotility and modulates macrophage function. Commun Biol. 2022 Aug 12;5(1):811.